

# Texture Based Quality Assessment of 3D Prints for Different Lighting Conditions

Jarosław Fastowicz and Krzysztof Okarma<sup>(✉)</sup>

Department of Signal Processing and Multimedia Engineering,  
Faculty of Electrical Engineering,  
West Pomeranian University of Technology, Szczecin,  
26. Kwietnia 10, 71-126 Szczecin, Poland  
{jaroslaw.fastowicz,krzysztof.okarma}@zut.edu.pl

**Abstract.** In the paper the method of “blind” quality assessment of 3D prints based on texture analysis using the GLCM and chosen Haralick features is discussed. As the proposed approach has been verified using the images obtained by scanning the 3D printed plates, some dependencies related to the transparency of filaments may be noticed. Furthermore, considering the influence of lighting conditions, some other experiments have been made using the images acquired by a camera mounted on a 3D printer. Due to the influence of lighting conditions on the obtained images in comparison to the results of scanning, some modifications of the method have also been proposed leading to promising results allowing further extensions of our approach to no-reference quality assessment of 3D prints. Achieved results confirm the usefulness of the proposed approach for live monitoring of the progress of 3D printing process and the quality of 3D prints.

**Keywords:** 3D prints · Image analysis · GLCM · Image quality assessment

## 1 Introduction

Growing popularity of the 3D printing technologies causes a great interest in applications of the 3D prints in various areas of science and technology. In various industrial applications four main types of technologies are utilized [9], namely inkjet printing, stereolithography, selective laser sintering and Fused Deposition Modelling (FDM) considered in this paper.

Observing growing interest in machine vision and image analysis applications for various areas of automation, robotics, mechatronics and other areas of industry, one of natural directions of their development is the visual feedback in the CNC machines [6] and 3D printers. An exemplary solution [3] used for the online defect detection in fused deposition of ceramics utilizes the comparison of process signatures for the captured images and the reference ones. Another vision based method [2], used for nondestructive monitoring the top surface of

the 3D print during printing, is based on the fuzzy model used for comparison of adjacent layers in order to identify the over- and under-filling.

In the paper [9] a monitoring system for 3D inkjet printer has been proposed which utilizes the neural networks for quality prediction of thin film electronic structures. The whole system is based on the measurement of resistivity without the direct use of cameras and comparison with a reference model is based on shape and geometrical properties.

Some other applications for vision based fault detection have also been provided by Szkilnyk [8] whereas the comparison of many other similar methods has been presented recently by Chauhan [1].

An initial study on the use of image analysis for automatic correction of detected errors in desktop 3D printers has been published by Straub [7]. The proposed system is based in five cameras and Raspberry Pi processing units and the images subjected to analysis are captured during numerous printing stops slowing the printing process. Unfortunately, this approach requires a precise calibration and is very sensitive to any disturbances including the camera motion and changes of lighting conditions. It allows the detection of “dry printing” caused by the lack of filament and premature termination of printing. The method utilize the comparison of the actual state of printing with the expected stage of the process and therefore can be considered as full-reference method.

A reliable quality assessment of images and textures is usually based on the comparison of some local features between two images. Recently, some interesting full-reference methods of texture similarity evaluation have been proposed [10, 11] which can be potentially useful also for evaluation of 3D prints. Nevertheless, the direct use of such methods would require the knowledge of the reference image and the perfect quality 3D print may be unavailable.

A still challenging problem is the automatic no-reference (“blind”) quality assessment of 3D prints based on the detection of structural faults, preferably in a continuous mode, and therefore such a need may be considered as the main motivation of this paper.

## 2 Proposed Method for Scanned 3D Prints

### 2.1 GLCM Analysis

Quality evaluation of scanned 3D prints should be based on the analysis of textures by means of their consistency. The reason for this assumption is that, following from the principle of operation of the 3D printers, the visible patterns generated by a 3D printer should be repetitive.

One of the most popular statistical approaches to texture analysis is the use of Haralick features [4] based on the Gray-Level Co-occurrence Matrix (GLCM). Such a matrix illustrates the spatial relations between the pixels in the specified neighborhood defined by the offset  $(\Delta x, \Delta y)$  and can be determined as:

$$C(i, j) = \sum_{p=1}^P \sum_{q=1}^Q \begin{cases} 1 & \text{if } A(p, q) = i \text{ and } A(p + \Delta x, q + \Delta y) = j \\ 0 & \text{otherwise} \end{cases} \quad (1)$$

where  $P = M - \Delta x$  and  $Q = N - \Delta y$ .

Each element of the GLCM ( $C(i, j)$ ) is calculated as the number of occurrences of pixels having the luminance level  $i$  in the specified neighborhood, defined by the offset  $(\Delta x, \Delta y)$ , with pixels of the luminance level  $j$ . In general four directions can be considered for each image: horizontal, vertical as well as  $45^\circ$  and  $135^\circ$  angles. Therefore 4 different matrices can be calculated for each specified distance (equal to one or more pixels).

Assuming the symmetrical definition of neighborhood, the luminance level  $i$  of a pixel above  $j$  is considered equally as  $i$  below  $j$  for the vertical GLCM. It leads to symmetrical GLCM, having even or zero values on its diagonal, used typically as the input data for the calculation of Haralick features [4]. For many natural images, as well as 3D prints considered in our paper, one may expect relatively high values near the diagonal of the GLCM due to anticipated high similarity of neighboring pixels.

Conducting the normalization of the GLCM by dividing of its elements by their sum, a convenient comparison of GLCM properties can be made, regardless of image resolution. The sum of elements can be easily predicted as for  $M$  rows and  $N$  columns, the sum of GLCM calculated for  $45^\circ$  and  $135^\circ$  angles is equal to  $(M - \Delta x) \cdot (N - \Delta y)$  whereas for the horizontal and vertical GLCM we obtain  $M \cdot (N - \Delta y)$  and  $(M - \Delta x) \cdot N$  respectively.

For the maximum dynamic luminance range of  $K$  levels, the GLCM matrix consisting of  $K \times K$  elements is obtained. For a typical 8-bit image with  $K = 256$  gray levels a reasonable compromise between the accuracy and the memory occupation, related also with computational complexity, seems to be the choice of  $K = 64$  levels as it has been assumed in further part of the paper. The experiments and calculations conducted using available 3D prints have confirmed the validity of such assumption as the use of  $K = 256$  levels has led to the same conclusions and obtained results are nearly identical.

## 2.2 Proposed Approach

As the GLCM is typically calculated for grayscale images and the distortions of 3D prints influence mainly the structural information, the typical color to grayscale conversion according to popular ITU recommendation BT.601-7 [5] has been assumed as the first preprocessing step. For such obtained grayscale image the vertical GLCM is calculated in order to check the repeatability of horizontal patterns which can be noticed in Fig. 1 illustrating exemplary test images used during experiments which have been obtained by scanning high quality 3D prints. The same calculations have been made for the images of distorted 3D prints as well (exemplary images are shown in Fig. 2). As mentioned above, all co-occurrence matrices have been calculated for  $K = 64$  levels and then chosen Haralick features have been determined. All the 3D prints have been obtained using two available 3D printers (RepRap Pro Ormerod 2 and Prusa i3) shown in Fig. 3.

In order to verify the experimental results several 3D prints have been prepared with some of them containing visible contaminations caused mainly by

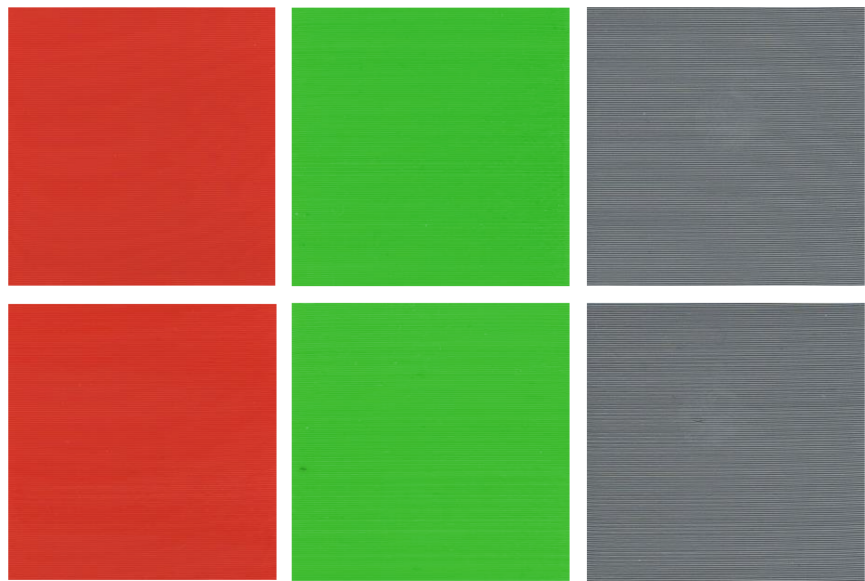


**Fig. 1.** Exemplary images obtained as scanned high quality 3D prints for different filaments

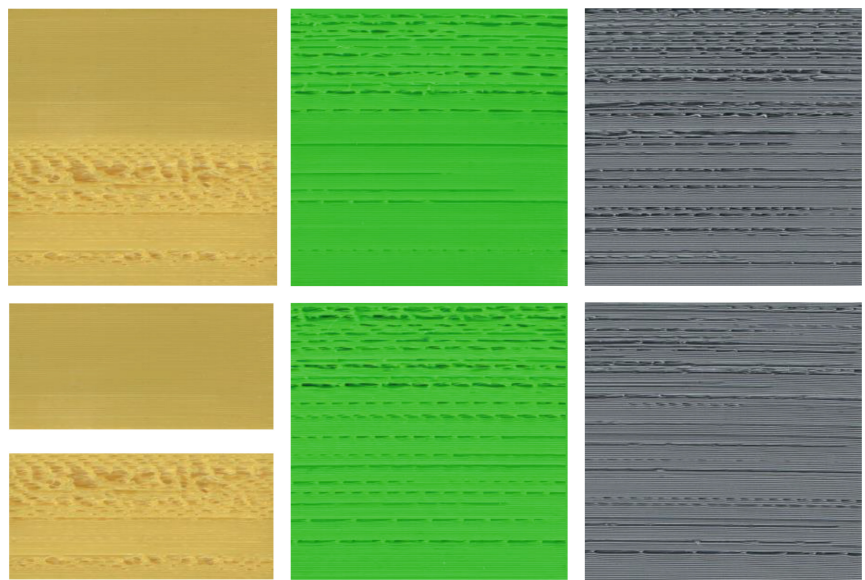


**Fig. 2.** Exemplary images obtained as scanned distorted 3D prints for different filaments (with partially high quality image on the left)

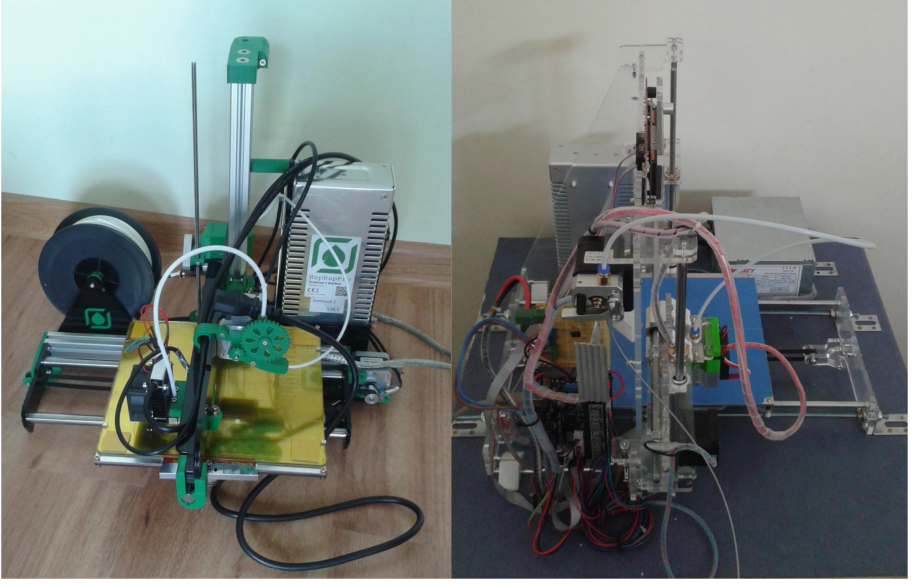


**Fig. 3.** Two FDM 3D printers used in experiments

the lack of filament. The presence of these distortions has been forced by manual change of the speed of filament's providing (slowing the feeder's drive) and simulation of clogged extruder.

However, due to the presence of some small distortions which in fact do not affect the quality of the 3D print, the results obtained for the GLCM calculated using the neighborhood defined by the offset equal to  $\Delta y = 1$  pixel are unsatisfactory and do not allow a proper estimation of 3D prints quality. Therefore, the proposed extension of such approach is based on the calculation of series of co-occurrence matrices and chosen Haralick features for different values of offset  $\Delta y$ . Analyzing the amplitude (regarded further as peak to peak value) and oscillating character of some features in dependence on the offset, a reliable classification of images representing higher and lower quality 3D scans can be made.

The most accurate results have been obtained using the homogeneity, measuring the closeness of the distribution of normalized symmetrical GLCM elements to its diagonal, which is defined as:

$$H = \sum_{i=1}^K \sum_{j=1}^K \frac{C_{i,j}}{1 + |i - j|} \quad (2)$$

according to documentation of MATLAB Image Processing Toolbox. It is closely related to Haralick's Inverse Difference Moment and the only difference is the definition of weights ( $1 + (i - j)^2$  is used in the denominator of the IDM instead

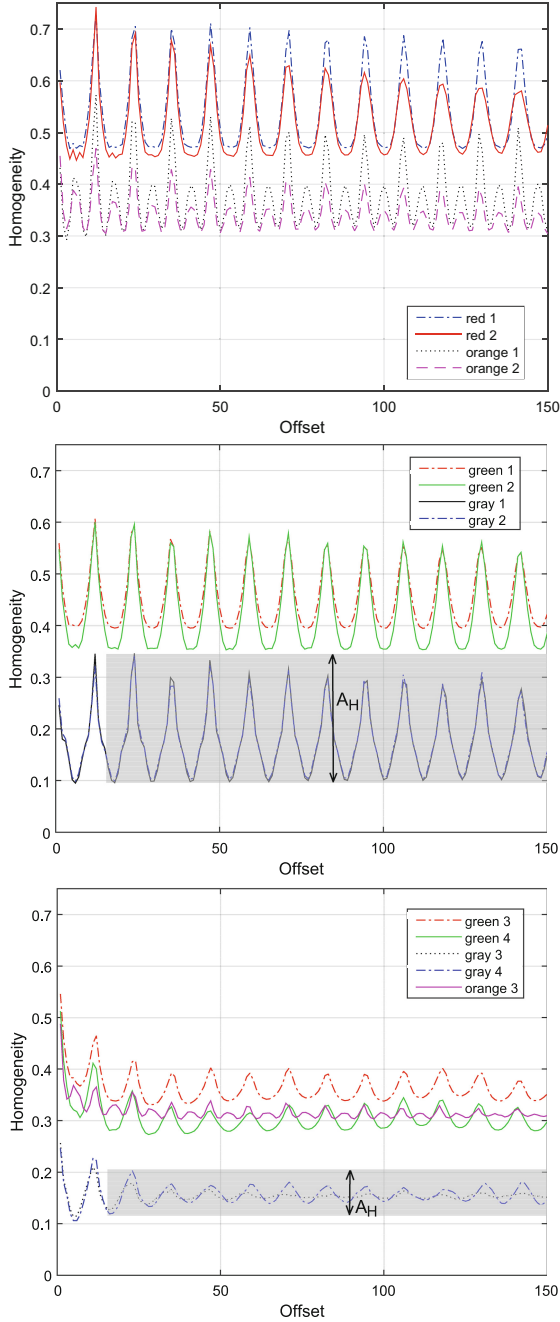


**Fig. 4.** Homogeneity plots obtained for the scanned different high quality (top and middle plots) and low quality 3D prints (bottom plots) with marked peak to peak homogeneity amplitude  $A_H$  for exemplary 3D prints

of  $1 + |i - j|$  used in homogeneity). Nevertheless, the obtained results are similar and do not affect the final conclusions.

### 2.3 Discussion of Experimental Results

Exemplary results of the vertical GLCM based homogeneity obtained for different 3D prints depending on the offset are shown in Fig. 4. Analyzing the plots presented in the same axis scales, it may be easily noticed that the amplitudes of oscillations of homogeneity  $A_H$  for low quality 3D prints are significantly lower, especially considering the offsets larger than 15 pixels in order to eliminate the influence of some minor distortions introduced during image acquisition. The peak to peak amplitude obtained for an exemplary image “orange 3” representing the low quality 3D print is equal to 0.0522 and the values of such amplitudes for the other scanned images are presented in Table 1.

**Table 1.** Peak to peak homogeneity amplitudes  $A_H$  calculated for the offsets greater than 15 pixels (as marked in Fig. 4) obtained for exemplary scans of 3D prints

High quality 3D prints							
Image	$A_H$	Image	$A_H$	Image	$A_H$	Image	$A_H$
red 1	0.2421	red 2	0.2407	orange 1	0.2226	orange 2	0.1288
green 1	0.1982	green 2	0.2429	gray 1	0.2498	gray 2	0.2436
Low quality 3D prints							
Image	$A_H$	Image	$A_H$	Image	$A_H$	Image	$A_H$
green 3	0.0855	green 4	0.0848	gray 3	0.0530	gray 4	0.0837

Lower absolute homogeneity values of orange prints as well as slightly lower oscillations both for high and low quality samples are caused by the semi-transparency of this filament illustrated in Fig. 5 where smartphone’s flashlight has been used as a light source. Lower absolute values of homogeneity, although still with relatively high oscillations for high quality 3D print, observed for gray samples result from some low frequency changes of brightness well visible in the upper right part of Fig. 1.

## 3 Application for Images Captured by the Camera

In practical applications, considering various shapes of 3D prints their scanning may be troublesome and much more desired solution would be a similar method based on the analysis of images captured by a camera, preferably even during the printing process. Such an approach could be useful for monitoring purposes allowing to stop the printing in case of presence of visible distortions on the surface of a 3D print. In more advanced version assuming fully visual feedback some detected distortions may be corrected during the printing process.



**Fig. 5.** Illustration of semi-transparency of some 3D prints for different types of PLA filaments illuminated from back side (orange, red, green and non-transparent gray). (Color figure online)

The application of the same procedure for the images captured by a camera illustrating the same 3D prints as in earlier experiments leads to the results presented in Fig. 6 and Table 2.

As can be easily noticed, the method proposed for the scanned images not always leads to satisfactory results since homogeneity amplitudes obtained for images acquired by a camera are usually lower both for high and low quality 3D prints. Their separation may be troublesome e.g. analyzing the homogeneity

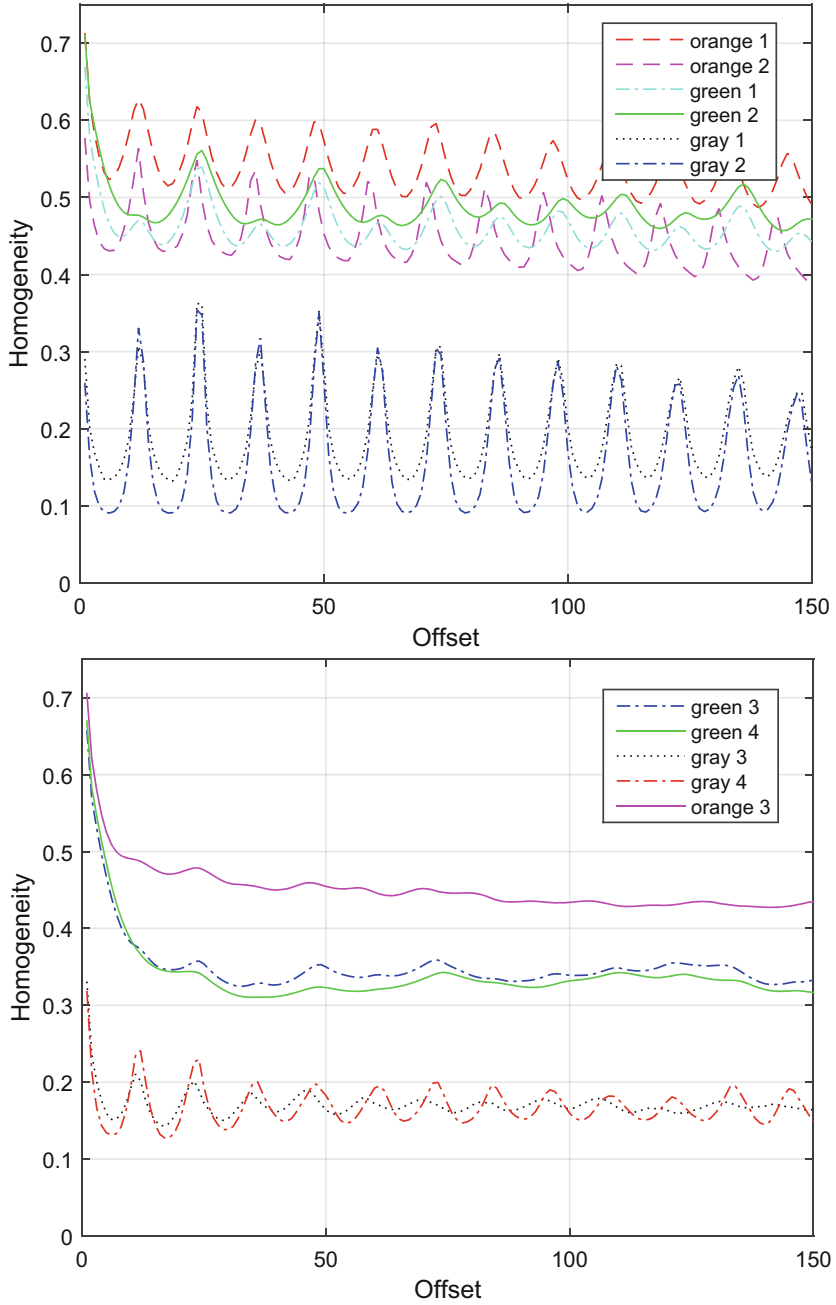


**Fig. 6.** Homogeneity plots obtained for selected high quality (upper plots) and low quality 3D prints (lower plots) captured by a camera

**Table 2.** Peak to peak homogeneity amplitudes  $A_H$  calculated for the offsets greater than 15 pixels obtained for exemplary captured images of 3D prints

High quality 3D prints							
Image	$A_H$	Image	$A_H$	Image	$A_H$	Image	$A_H$
red 1	0.2126	red 2	0.2400	orange 1	0.1308	orange 2	0.1605
green 1	0.1093	green 2	0.1038	gray 1	0.2304	gray 2	0.2633
Low quality 3D prints							
Image	$A_H$	Image	$A_H$	Image	$A_H$	Image	$A_H$
green 3	0.0340	green 4	0.0363	gray 3	0.0588	gray 4	0.1023

obtained for the images “green 1” and “green 2” in comparison to “orange 1” and “orange 2”.

Nevertheless, the quality estimation of the 3D prints based on images captured by a camera may be based on both homogeneity amplitude and its mean value for different offsets. As it has been verified experimentally, high peak to peak homogeneity amplitude (over 0.15) denotes high quality of the 3D print whereas low homogeneity amplitude (under 0.07) denotes the presence of distortions. For its medium values (between 0.07 and 0.15) the mean values should be considered which are much lower for low quality samples (about 0.2) whereas for the high quality 3D prints obtained values are over 0.4 with high amplitude of oscillations.

## 4 Additional Detection of Image Type

In order to ensure a better universality of the proposed approach the additional detection of the image type may be considered. Consequently it allows the use of the simplified approach for scanned images or images obtained by a camera in relatively more uniform lighting conditions (e.g. professional 3D printers with closed casings). For such images a threshold value of homogeneity peak to peak amplitude about 0.12 should allow proper classification of 3D prints. For the images captured in non-uniform lighting conditions, typical for home use 3D printers, a lower threshold dependent on the average homogeneity value can be used.

The detection of the image type and classification into two classes (scanned images and photos) can be implemented utilizing the correlation values calculated for the GLCM. The presence of relatively high negative correlation values is characteristic for the scanned images whereas for the images acquired by a camera those values are always positive or can be characterized by several times smaller negative peaks in comparison to positive ones as shown in Fig. 7.

For the scanned images the average values of the correlation for the offsets greater than 15 pixels are either negative or very small positive values (below 0.1) whereas for images acquired by a camera those values are much higher (over 0.1)

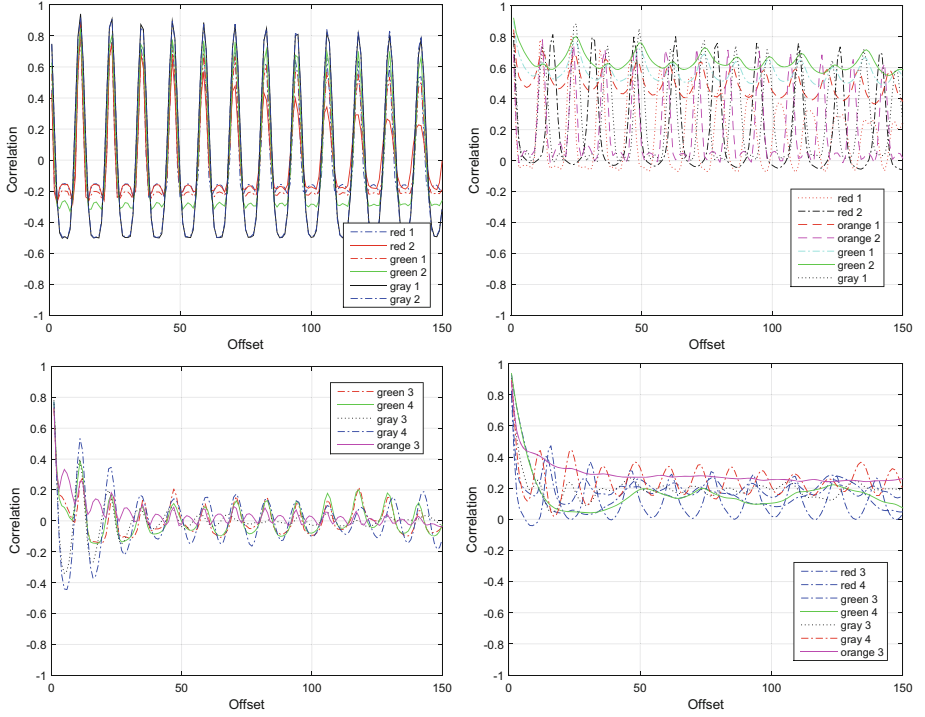


**Fig. 7.** Correlation plots obtained for selected scanned images (left plots) and photos acquired by a camera (right plots) captured by a camera (images obtained for high quality 3D prints in the top row)

and always positive. As can be observed such approach is generally valid both for high quality 3D prints as well as in the presence of distortions lowering the quality.

## 5 Conclusions

Presented results confirm the usefulness of the proposed method of quality evaluation of 3D prints based on scanned images or photos captured by cameras. For all tested samples the proposed metric based on the amplitude of homogeneity calculated for vertical GLCM, together with its mean value for images acquired by cameras, has led to very promising results. Proposed method of determining the image type, based on the correlation calculated for the vertical GLCM as well, allows the choice of the proper version of the method in the second stage.

Comparing the results obtained for high and low quality 3D prints made from the same filament, lowering the mean values and the amplitude of homogeneity can be noticed. Nevertheless, in practical applications related to live monitoring of the 3D printing, a comparison of parameters with previously made high quality

3D print based on the same filament may be troublesome and would require a calibration of the system's parameters after each change of the filament type. Therefore, such a method can be considered rather as a full-reference approach than a "blind" quality evaluation without comparison to any images of perfect quality 3D prints.

Observing the influence of semi-transparency of different filaments an interesting relation between the transparency level and the mean value of homogeneity calculated for the vertical GLCM may be noticed. Therefore, our future research will be concentrated on the improvements of the proposed approach towards fully automated no-reference quality assessment of 3D prints for different types of filaments. Another direction of future research will be related to experiments with some other shapes of printed 3D objects in order to improve the universality of the proposed method.

## References

1. Chauhan, V., Surgenor, B.: A comparative study of machine vision based methods for fault detection in an automated assembly machine. *Procedia Manufact.* **1**, 416–428 (2015)
2. Cheng, Y., Jafari, M.A.: Vision-based online process control in manufacturing applications. *IEEE Trans. Autom. Sci. Eng.* **5**(1), 140–153 (2008)
3. Fang, T., Jafari, M.A., Bakhadyrov, I., Safari, A., Danforth, S., Langrana, N.: Online defect detection in layered manufacturing using process signature. In: *Proceedings of IEEE International Conference on Systems, Man and Cybernetics*, San Diego, California, USA, vol. 5, pp. 4373–4378, October 1998
4. Haralick, R.M., Shanmugam, K., Dinstein, I.: Textural features for image classification. *IEEE Trans. Syst. Man Cybern.* **3**(6), 610–621 (1973)
5. ITU-T: Recommendation BT.601-7 - Studio encoding parameters of digital television for standard 4: 3 and wide-screen 16: 9 aspect ratios (2011)
6. Okarma, K., Grudziński, M.: The 3D scanning system for the machine vision based positioning of workpieces on the CNC machine tools. In: *Proceedings of 17th International Conference Methods and Models in Automation and Robotics (MMAR)*, Międzyzdroje, Poland, pp. 85–90, August 2012
7. Straub, J.: Initial work on the characterization of additive manufacturing (3D printing) using software image analysis. *Machines* **3**(2), 55–71 (2015)
8. Szkilnyk, G., Hughes, K., Surgenor, B.: Vision based fault detection of automated assembly equipment. In: *Proceedings of ASME/IEEE International Conference on Mechatronic and Embedded Systems and Applications*, Parts A and B, Washington, DC, USA, vol. 3, pp. 691–697, August 2011
9. Tourloukis, G., Stoyanov, S., Tilford, T., Bailey, C.: Data driven approach to quality assessment of 3D printed electronic products. In: *Proceedings of 38th International Spring Seminar on Electronics Technology (ISSE)*, Eger, Hungary, pp. 300–305, May 2015
10. Žujović, J., Pappas, T.N., Neuhoff, D.L.: Structural similarity metrics for texture analysis and retrieval. In: *Proceedings of 16th IEEE International Conference on Image Processing (ICIP)*, Cairo, Egypt, pp. 2225–2228, November 2009
11. Žujović, J., Pappas, T.N., Neuhoff, D.L.: Structural texture similarity metrics for image analysis and retrieval. *IEEE Trans. Image Process.* **22**(7), 2545–2558 (2013)

Computer Vision and Graphics

International Conference, ICCVG 2016, Warsaw, Poland,

September 19-21, 2016, Proceedings

Chmielewski, L.J.; Datta, A.; Kozera, R.; Wojciechowski, K.  
(Eds.)

2016, XIII, 658 p. 330 illus., Softcover

ISBN: 978-3-319-46417-6